APPROVED FOR PUBLIC RELEASE
DISTRIBUTION UNLIMITED

TECHNICAL NOTE NO. 72-3

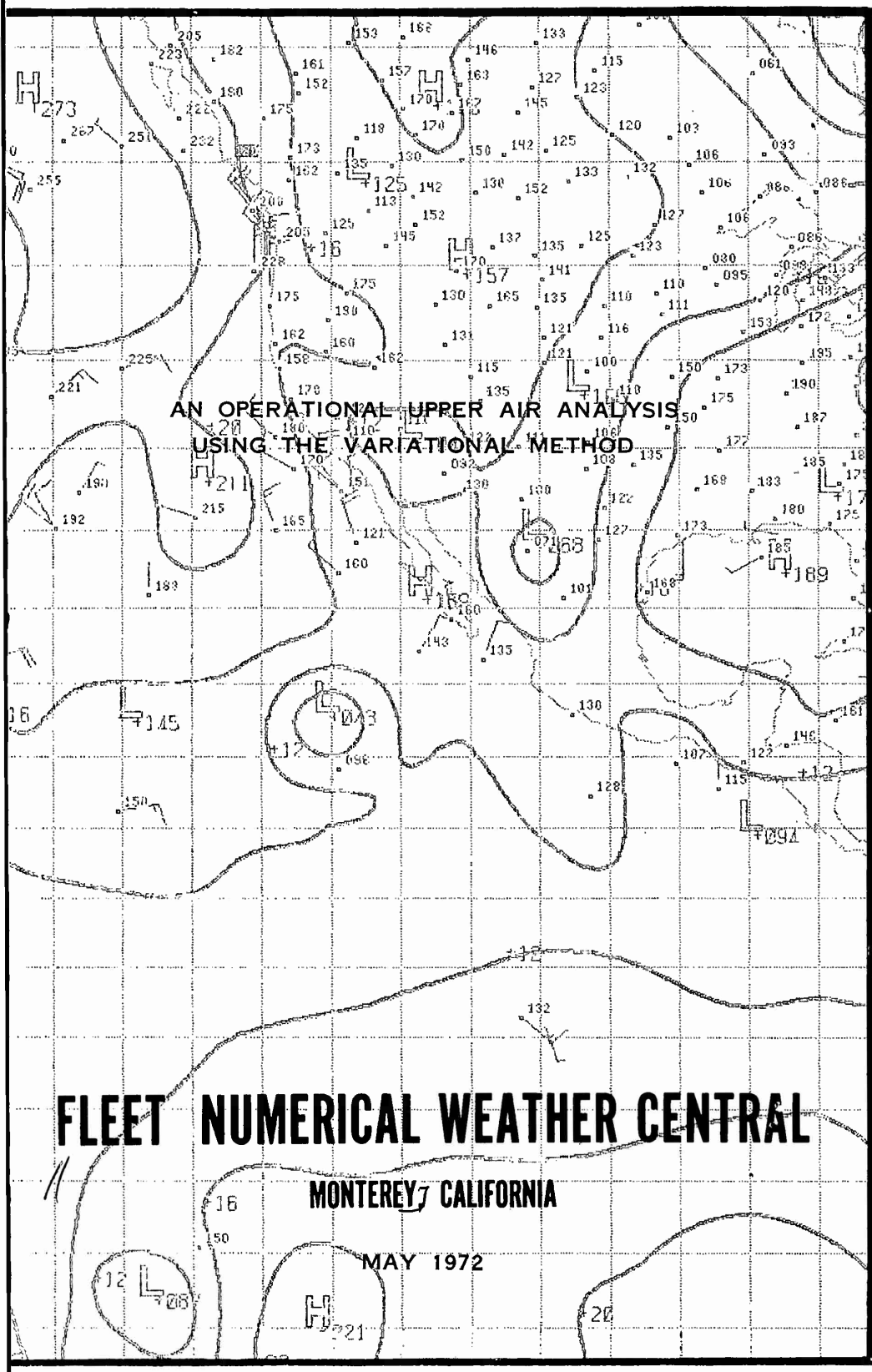

AN OPERATIONAL UPPER AIR ANALYSIS USING THE VARIATIONAL METHOD

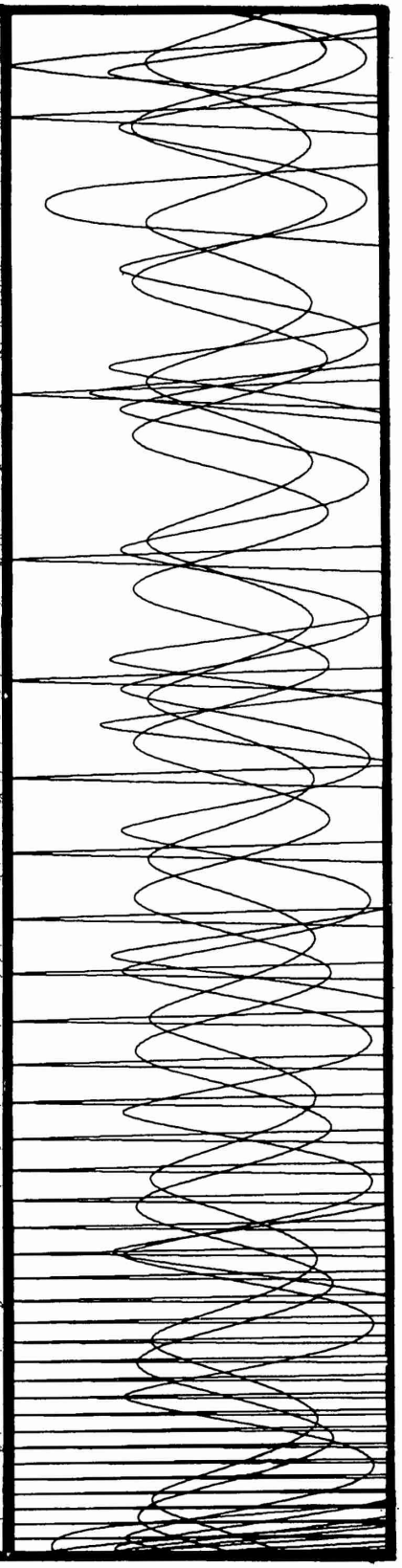

FLEET NUMERICAL WEATHER CENTRAL

MONTEREY, CALIFORNIA

MAY 1972

AN (1) AD- 745 364
CS (2) 040200
CL (3) (U)
CA (5) FLEET NUMERICAL WEATHER CENTRAL MONTEREY CALIF
TI (6) An Operational Upper Air Analysis using the Variational Method.
TC (8) (U)
DN (9) Technical note.
AU (10) Lewis,John M.
RD (11) May 1972
PG (12) 48p
RS (14) TN-72-3
RC (20) Unclassified report
DE (23) (*atmospheric motion, troposphere), (*weather forecasting, marine meteorology), WIND, ATMOSPHERIC TEMPERATURE, AIR MASS ANALYSIS, METEOROLOGICAL CHARTS, TROPICAL REGIONS, NUMERICAL ANALYSIS, PACIFIC OCEAN
DC (24) (U)
ID (25) north pacific ocean, numerical weather forecasting
IC (26) (U)
AB (27) An upper air objective analysis of wind and temperature has been developed for operational use at Fleet Numerical Weather Central. The primary feature of this analysis scheme is the vertical and horizontal extrapolation of information into the data-sparse regions from the data-rich surface and jet aircraft level. The extrapolation is based on Sasaki's recent extensions of the variational analysis method. The hydrostatic equation and horizontal momentum equations are used as dynamical constraints and these equations are combined to relate temperature and wind through a generalized thermal wind relationship. The governing analysis equations are elliptic and amenable to solution by the relaxation process. Vertical coupling of both wind and temperature is demonstrated through the detailed examination of a case study in the North Pacific. (Author)
AC (28) (U)
DL (33) 01
CC (35) 138670

AN OPERATIONAL UPPER AIR ANALYSIS USING THE VARIATIONAL METHOD

Technical Note No. 72-3

May 1972

by

J. M. Lewis

FOREWORD

This technical note describes the Numerical Variational Analysis (NVA) program used at FNWC Monterey to prepare upper air analyses of wind and temperature for the Global Band Grid. The grid has a mesh length of 2.5 degrees at the Equator and extends around the world covering latitudes between 40S and 60N. (The tropical grid used at FWC Pearl Harbor is a subset of this one.)

The program is unique to Naval Weather Service analysis effort in the tropics in that it couples wind and temperature through thermal wind constraints thereby automatically ensuring vertical consistency. It is designed to make maximum use of all source data--especially over sparsely sampled ocean areas.

Reviewed and approved on 20 May 1972.

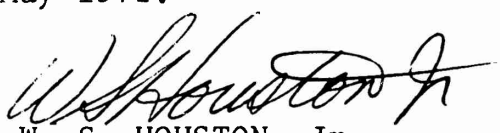

W. S. HOUSTON, Jr.
Captain, U. S. Navy
Commanding Officer
Fleet Numerical Weather Central

TABLE OF CONTENTS

LIST OF FIGURES AND TABLES

Page

Tables

ABSTRACT

An upper air objective analysis of wind and temperature has been developed for operational use at Fleet Numerical Weather Central. The primary feature of this analysis scheme is the vertical and horizontal extrapolation of information into the data-sparse regions from the data-rich surface and jet aircraft level. The extrapolation is based on Sasaki's recent extensions of the variational analysis method. The hydrostatic equation and horizontal momentum equations are used as dynamical constraints and these equations are combined to relate temperature and wind through a generalized thermal wind relationship. The governing analysis equations are elliptic and amenable to solution by the relaxation process. Vertical coupling of both wind and temperature is demonstrated through the detailed examination of a case study in the North Pacific.

1. INTRODUCTION

The synoptic analysis of meteorological fields at mid-tropospheric levels has been plagued by the scarcity of conventional data. The data coverage over the densely populated continents of Europe and North America has generally been adequate for the definition of the large-scale or extra-tropical cyclone features. For ocean operations, however, the conventional data is strikingly inadequate to define even these large-scale features. To augment the information at these mid-levels, the relatively rich sources of data at the surface have been used. Yanai (1964) achieved a considerable improvement over standard methods when he relied heavily upon the surface data to build upper-air analyses of wind in the Caribbean. His success stemmed from the ability to construct an accurate surface wind analysis from relatively abundant ship and island reports. Adjoining upper air charts were then built stepwise by differential analysis using the successive corrections method (SCM), an operationally attractive scheme formulated by Bergthórsson and Döös (1955) and modified by Cressman (1959).

Another approach that has been successful at the National Hurricane Research Laboratory (NHRL) is the layer mean analysis. In this analysis, the data base for the lower troposphere (1000 - 600 mb) and the upper troposphere (600 - 200 mb)

is effectively increased by amalgamating the information from the individual mandatory levels. The apparent success of this scheme is based on the two-layer structure of the tropics during most of the year (Wise and Simpson, 1971).

In addition to increasing the data base for each meteorological variable, the ability to couple variables through dynamical or empirical relations is germane to analysis in data-sparse regions. Thus, the observation of a particular variable can indirectly produce information about another variable. Sasaki (1958, 1969) has developed a scheme based on variational calculus which couples the meteorological fields by constraining the analysis to satisfy a governing set of diagnostic or prognostic equations. This methodology has been used at Fleet Numerical Weather Central (FNWC) to produce surface winds and pressure on a global-band grid which encompasses the tropical belt (Lewis and Grayson, 1972). The work of Yanai (1964) also coupled the fields at the surface by using a statistical-dynamical model proposed for use at the Japan Meteorological Agency (JMA) and reported by Masuda and Arakawa (1962).

The coupling of data in upper-air analysis has received considerable attention in recent years. This interest has been stimulated by the necessity to define observational networks for numerical weather prediction (Döös, 1970). The

operational centers have traditionally used geostrophic theory in conjunction with the successive corrections method. With upsurge in global forecasting, however, the analysis techniques have incorporated ageostrophic effects. The National Meteorological Center (NMC) now analyzes heights and winds by spectral methods which use Hough functions (eigenfunctions of Laplace's tidal equation) for horizontal modes and empirical orthogonal functions for the vertical modes (Flattery, 1971). The results indicate that reasonable height and wind fields are obtained, even at the equator. Since the Hough functions are derived from equations which neglect the nonlinear advection terms in the momentum equations, there have been some problems when the analysis is used for initializing the primitive equation forecast model (Flattery, 1970). Gradient wind corrections have been made in an attempt to account for the nonlinear imbalance.

The proposed upper-air analysis scheme at FNWC is designed for operational use on a global band grid extending from 40S to 60N which has a mesh length of 150 n mi at the equator and 75 n mi at 60N. The change of mesh size is a consequence of the distortion inherent in the Mercator secant projection (true at 22.5N and 22.5S) used for the analysis. The flight support for turbo-prop aircraft has been a primary consideration in the development of this scheme. These planes cruise

in the vicinity of the 400 mb surface and flight support and guidance at this level are necessary. As mentioned previously, the data-rich levels are the surface and the jet aircraft level (vicinity of 250 mb). The extrapolation of data from these data-abundant regions into the mid-troposphere is accomplished by using Sasaki's numerical variational analysis (NVA) method. This approach reduces the analysis problem to a boundary value problem where the upper and lower surface are specified and the interior is determined subject to the governing elliptic analysis equations. Since there are scattered observations between the surface and 250 mb, the analysis scheme must have the capability of weighting this local information as well as incorporating the extrapolated information. The variational analysis scheme provides a natural way to accommodate both the observations and the dynamically extrapolated information.

The surface analysis which is used to provide boundary values for the upper-air analysis is based on the operational scheme reported by Lewis and Grayson (1972). This analysis has been subjected to a two-dimensional adjustment by NVA. The momentum equations used as constraints for this surface analysis are consistent with the upper-air scheme except that they contain the effects of surface friction. The 250 mb analysis is found by the SCM. A two-dimensional

adjustment could be performed at this level, but has been postponed until the general features of the extrapolation procedure are clarified. In order to incorporate dynamical information at this level, the forecasted wind from the FNWC primitive equation model (Kesel and Winninghoff, 1971) is used as the guess field for the SCM between 20N - 60N.

Since aircraft rarely report geopotential (D-values) and, moreover, because of the limited credibility of these observations, the coupling of temperature and wind has been used to build the upper-air analyses. The subjective or manual analysis of upper-air wind has heavily relied upon this coupling or thermal wind relationship (see Saucier, 1955). In order to couple these fields over the tropics and extratropical regions, a more general form of the thermal wind relation which includes ageostrophic effects must be employed. Forsythe (1945) developed graphical techniques which enabled the hand-analyst to account for ageostrophic effects between the temperature gradient and wind shear. It is precisely this traditional synoptic rule connecting temperature gradient and wind shear that provides the vehicle for extrapolation in the objective scheme.

2. BASIC INGREDIENTS FOR THIS ANALYSIS, OBSERVATIONS AND THE GENERAL THERMAL WIND RELATION

The operational approach to numerical variational analysis (referred to as NVA in future discussion) adopted at FNWC is: (1) irregularly distributed observations of each variable are independently interpolated to grid points by the SCM, (2) a reliability is attached to the variable at each grid point and is dependent upon both the number of observations affecting this point and the distance of the observations from the point, and (3) an adjustment of the "observations" (the analysis resulting from the SCM) by the NVA equations which have incorporated the model constraints.

The analysis is performed every 6 hr and the natural candidate for the guess field of SCM is the previous analysis or, equivalently stated, the 6 hr persistence field. In addition to the persistence field, however, the FNWC primitive equation model produces a forecast every 12 hr over the Northern Hemisphere. The guess field for the wind is 6 hr persistence south of 20N. Between 20N - 60N, the 6 hr and 12 hr forecasts are alternately used. That is, the 06 GMT and 18 GMT global-band analyses use the 6 hr forecasts from 00 GMT and 12 GMT, respectively. Similarly, the 00 GMT and 12 GMT analyses use 12 hr forecasts from 12 GMT (previous day) and 00 GMT, respectively. The temperature guess field,

however, is strictly the 6 hr persistence field. The feedback from wind to temperature occurs in the NVA scheme. Only when the "observations" (SCM analyses) are independent can the variational adjustment process guarantee maximum likelihood estimates (Cramér, 1955; Lewis and Grayson, 1972).

Four successive scans are made to correct the guess field. For the analysis of temperature, the radii are 600, 300, 200 and 100 n mi, respectively. Grid points which are 600 n mi or further from a report are unmodified, i.e., the 6 hr persistence becomes the current analysis. It is precisely this kind of event that often causes the SCM to produce "unmeteorological" fields, i.e., the data-sparse areas adjoining the data-rich areas show discontinuities which are characteristic of the mathematical weighting functions of the SCM and are not attributable to meteorological events.

In a similar fashion, three scans are used by the SCM for wind analysis. Here the two component directions are analyzed together. In addition to speeding the analysis procedure, the decision to accept or reject wind data is based on the vector rather than the separate scaler components. The radii for the wind analysis are 450, 300 and 150 n mi, respectively. The successively decreasing scan radii are designed to capture the larger scale features on the preliminary

scan and then include the smaller scale features on the following scans. Stephens (1967) has discussed the relationship between characteristic meteorological scale and the scan radii under the assumption of uniformly distributed data.

The second ingredient to NVA is the model dynamics which will be used to couple the variables and provide the path to extrapolation from the data-dense to data-sparse regions. The governing equations are modified in a manner consistent with the NVA at the surface (Lewis and Grayson, 1972). Namely, the nonlinear advection terms are approximated by the distributions resulting from the SCM. The primary advantage is the simplification of the Euler equations and the guarantee of an elliptic differential equation system regardless of the weights used in the variational formulation. The guaranteed ellipticity leads to rapid convergence when the relaxation process is used. The governing equations in Mercator coordinates are:

$$\frac{\partial u}{\partial t} + \tilde{W}\cdot\nabla\tilde{u} - fv = -m\frac{\partial \phi}{\partial x} \tag{1}$$

$$\frac{\partial v}{\partial t} + \tilde{W}\cdot\nabla\tilde{v} + fu = -m\frac{\partial \phi}{\partial y} \tag{2}$$

$$\frac{\partial \phi}{\partial \sigma} = RT \tag{3}$$

$$\sigma = \ln (p_o/p) \tag{4}$$

where: t : time

x : east-west coordinate (positive eastward)

y : north-south coordinate (positive northward)

σ : vertical coordinate (positive upwards)

$\mathbb{V} = u\hat{i} + v\hat{j}$: horizontal velocity

$\hat{i}$: unit vector along positive x

$\hat{j}$: unit vector along positive y

$\tilde{\mathbb{V}} = \tilde{u}\hat{i} + \tilde{v}\hat{j}$: velocity from SCM

T : temperature

ϕ : geopotential

f : Coriolis parameter

$m = \cos\theta_o \sec\theta$: image scale factor for Mercator projection true at 22.5N and 22.5S

θ : latitude (θ_o = 22.5 degrees)

p_o : reference pressure (1013 mb)

R : gas constant for dry air

$\nabla = m \frac{\partial(\ )}{\partial x} \hat{i} + m \frac{\partial(\ )}{\partial y} \hat{j}$: gradient operator

To simplify the notation, the nonlinear advection terms are denoted by:

$$\tilde{A} = \tilde{\mathbb{V}} \cdot \nabla \tilde{u} \tag{5}$$

$$\tilde{B} = \tilde{\mathbb{V}} \cdot \nabla \tilde{v} \tag{6}$$

The general thermal wind relation is derived by eliminating the geopotential from the momentum equations, (1) and (2),

by substituting from the hydrostatic equation, (3). In component form, this relation is

$$\frac{\partial}{\partial t}\left(\frac{\partial u}{\partial \sigma}\right) = -\frac{\partial}{\partial \sigma}\tilde{A} + f\frac{\partial v}{\partial \sigma} - mR\frac{\partial T}{\partial x} = F \tag{7}$$

$$\frac{\partial}{\partial t}\left(\frac{\partial v}{\partial \sigma}\right) = -\frac{\partial}{\partial \sigma}\tilde{B} - f\frac{\partial u}{\partial \sigma} - mR\frac{\partial T}{\partial y} = G \tag{8}$$

where the separation of terms by functions F and G will prove useful in the discussion on minimization.

3. THE VARIATIONAL FORMULATION AND ASSOCIATED EULER EQUATIONS

The timewise localized version of NVA (Sasaki, 1970) is adopted for the upper-air analysis and the functional to be minimized assumes the form:

$$I = \iiint_{V} \{ [\tilde{\alpha}(u-\tilde{u})^2 + \tilde{\alpha}(v-\tilde{v})^2] + [\tilde{\beta}(T-\tilde{T})^2] + [\alpha(\frac{\partial}{\partial t}(\frac{\partial u}{\partial \sigma}))^2 + \alpha(\frac{\partial}{\partial t}(\frac{\partial v}{\partial \sigma}))^2] \} J(\frac{x_e, y_e}{x, y}) \, dV \tag{9}$$

where

$\tilde{\alpha}$: Gauss' precision modulus for wind

$\tilde{\beta}$: Gauss' precision modulus for temperature

α : Dynamical weight

x_e : east-west coordinate on earth

y_e : north-south coordinate on earth

$(\tilde{})$: analysis resulting from the SCM

$J(\frac{x_e, y_e}{x, y})$: Jacobian of transformation from earth to Mercator coordinates

dV : incremental volume ($dxdyd\sigma$)

The relationship between earth and map coordinates is

$$dx_e dy_e = J(\frac{x_e, y_e}{x, y}) \, dxdy \, . \tag{10}$$

Consequently, (9) implies that equal weight is given to

equal earth areas, not equal map areas. For the Mercator projection,

$$J\left(\frac{x_e, y_e}{x, y}\right) = m^{-2} \tag{11}$$

By virtue of (7) and (8), the functional can be rewritten

$$I = \iiint_{\mathcal{V}} \left\{ \begin{array}{l} \tilde{\alpha}[(u-\tilde{u})^2 + (v-\tilde{v})^2] \\ + \tilde{\beta}[(T-\tilde{T})^2] \\ + \alpha[F^2 + G^2] \end{array} \right\} J\left(\frac{x_e, y_e}{x, y}\right) d\mathcal{V} \tag{12}$$

The first set of bracketed terms force the analysis toward the SCM velocity in proportion to $\tilde{\alpha}$. Similarly, the second bracketed term forces the temperature toward the SCM temperature in proportion to $\tilde{\beta}$. The weights $\tilde{\alpha}$ and $\tilde{\beta}$ are called observational weights or Gauss' precision moduli and specified beforehand, i.e., before the minimization process. They are a measure of the confidence in the respective SCM fields. Following the discussion of these weights in the paper by Lewis and Grayson (1972), let

$$\tilde{\alpha} = 1/\sigma_W \ , \ \tilde{\beta} = 1/\sigma_T \tag{13}$$

where σ_W is the mean-square difference between the separate wind components of NVA and SCM and σ_T is the mean-square difference between the NVA and SCM temperatures.

In analogy with the observational weights $\tilde{\alpha}$ and $\tilde{\beta}$, the dynamical weight α is expressed as

$$\alpha = 1/\sigma_t \qquad (14)$$

where σ_t is the mean-square value of local time rate of change of wind shear as calculated from (7) and (8). Alternatively stated, α is a measure of the steadiness or degree with which u, v, and T satisfy F = G = 0. As α increases, the analyzed fields are forced closer to the steady state relationships.

The observational weights $\tilde{\alpha}$ and $\tilde{\beta}$ should be a function of space (and time) and generally distinguish between (1) grid points that benefited from nearby observations and (2) grid points unaffected by observations and consequently reflecting 6 hr persistence after the SCM analysis. A method for specification of $\tilde{\alpha}$ and $\tilde{\beta}$ in terms of the distance-dependent weighting implicit in the SCM has been discussed by Lewis and Grayson (1972). During the development stages of the upper air analysis, the weights have not varied as a function of space but have been chosen to reflect only typical variance of the wind and temperature.

As mentioned in the Lewis and Grayson (1972) paper, the separately specified values of σ_w, σ_T and σ_t are not preserved in the minimization process. However, the ratios between these values are preserved. This fact will be obvious when the Euler equations (Eqs. 17-19) are examined. If a, b and c are chosen for σ_w, σ_T and σ_t, the final analysis produces

values d, e and f, respectively, where a:b:c = d:e:f. Rather than specifying σ_w, σ_T and σ_t, it is sufficient to specify σ_w/σ_t and σ_T/σ_t.

A necessary and sufficient condition for minimization of (12) is the vanishing of the first variation, denoted by δI. The sufficiency of this condition is directly attributable to the quadratic nature of the integrand (Lanczos, 1970, p. 41). Using integration by parts and the commutative properties of the δ-process (Lanczos, 1970, p. 56), the functional takes the form

$$0 = \delta I = \iiint_{\mathcal{V}} (P\delta u + Q\delta v + W\delta T)\, d\mathcal{V} + \{\text{terms evaluated on surface boundaries}\} . \quad (15)$$

The expressions P, Q and W are differential expressions which will be explicitly written later.

The boundary terms indicated on the right-hand side of (15) involve integrals over the bounding surfaces, viz., the walls at 40S and 60N, the 250 mb level and the earth's surface. The east-west boundaries are cyclic because of the 360° longitudinal span of the analysis region. The conditions necessary to cause these integrals to vanish are called the natural boundary conditions. There is generally more than one set of acceptable boundary conditions. The simplest boundary conditions are: $\delta T = 0$ on the north and south walls and $\delta u = \delta v = 0$ along the upper and lower surfaces.

These are Dirichlet conditions and allow no adjustment of temperature and velocity along the boundaries where the respective variations vanish. Alternative boundary conditions can be found by examination of the integrals given in the appendix. The simplicity of the Dirichlet conditions, especially in regard to the programming of numerical methods for solution, has led to the adoption of this set of boundary conditions.

Having disposed of the terms evaluated on the surface boundaries and because of the independence of the variations of u, v and T, the solution to (15) is

$$P = Q = W = 0 \tag{16}$$

where

$$P = \left\{ \begin{array}{l} f^2 \frac{\partial^2 u}{\partial \sigma^2} - (\frac{\tilde{\alpha}}{\alpha})(u-\tilde{u}) \\ \\ + mfR \frac{\partial}{\partial \sigma} (\frac{\partial T}{\partial y}) + f \frac{\partial^2 \tilde{B}}{\partial \sigma^2} \end{array} \right\} = 0 \tag{17}$$

$$Q = \left\{ \begin{array}{l} f^2 \frac{\partial^2 v}{\partial \sigma^2} - (\frac{\tilde{\alpha}}{\alpha})(v-\tilde{v}) \\ \\ - mfR \frac{\partial}{\partial \sigma} (\frac{\partial T}{\partial x}) - f \frac{\partial^2 \tilde{A}}{\partial \sigma^2} \end{array} \right\} = 0 \tag{18}$$

$$W = \left\{ \begin{array}{l} \overset{①}{\nabla\cdot(m^{-2}\nabla T)} - \overset{②}{(mR)^{-2}\,(\frac{\tilde{\beta}}{\alpha})(T-\tilde{T})} \\ \\ \underset{③}{-\frac{\hat{k}}{m}\cdot\nabla\times(\frac{f}{mR}\frac{\partial W}{\partial\sigma})} + \underset{④}{\nabla\cdot(\frac{\mathbb{C}}{m^2R})} \end{array} \right\} = 0 \qquad (19)$$

and

$$\mathbb{C} = \frac{\partial\tilde{A}}{\partial\sigma}\,\hat{i} + \frac{\partial\tilde{B}}{\partial\sigma}\,\hat{j} \quad . \qquad (20)$$

The local vertical unit vector is $\hat{k}$ and the dot and cross-products have been incorporated in (19). Equations (17) and (18) can be combined to produce the vector representation:

$$\left\{ \begin{array}{l} \overset{①}{f^2\frac{\partial^2 W}{\partial\sigma^2}} - \overset{②}{(\frac{\tilde{\alpha}}{\alpha})(W-\tilde{W})} \\ \\ \underset{③}{+ fR\hat{k}\times\frac{\partial}{\partial\sigma}\nabla T} - \underset{④}{f\hat{k}\times\frac{\partial}{\partial\sigma}\mathbb{C}} \end{array} \right\} = 0 \quad . \qquad (21)$$

The equations, (17)-(19), or equivalently, (19) and (21), are called The Euler equations. Together with the Dirichlet boundary conditions, they constitute the governing equations for the upper-air analysis.

The derivation of (17)-(19) has assumed that α is invariant in space. A variable α can easily be included in the equations, but the applicability of the model constraints over the entire analysis region dictates the constancy. The ratios $\tilde{\beta}/\alpha$ and

$\tilde{\alpha}/\alpha$ are the controlling factors in (19) and (21), respectively. As the reliabilities of the SCM wind and temperature increase, the ratios $\tilde{\alpha}/\alpha$ and $\tilde{\beta}/\alpha$ increase, respectively. Consequently, term ② in both (19) and (21) forces the analysis toward the SCM analysis in proportion to these ratios.

Terms ① and ③ in (21) represent the geostrophic coupling between wind and temperature. In fact, except for the differentiation with respect to σ, this is the geostrophic thermal-wind relationship. Interpreted physically, the vertical change of horizontal temperature gradient contributes to the curvature, $\frac{\partial^2 W}{\partial \sigma^2}$, of the wind profile. Term ④ brings the nonlinear advection of momentum into the process and is generally an important contributer in the regions of strong horizontal shear such as in the area neighboring the jet stream. Although this term is approximated by the SCM analysis, the approximation is improved by a "re-cycling" technique explained in the next chapter.

The horizontal curvature of temperature, $\nabla^2 T$, and the vertical variation of vorticity, $\frac{\partial}{\partial \sigma}(\hat{k} \cdot \nabla \times W)$, are related by terms ① and ③ in (19). Again, these terms stem from a strict hydrostatic-geostrophic balance. The nonlinear advective effects are contained in ④ and are associated with vertical variation of streamline curvature as expressed by $u \frac{\partial}{\partial \sigma}(\frac{\partial^2 u}{\partial x^2})$, etc. These nonlinear terms are subject to

improved approximation by the re-cycling method mentioned above.

In the development of the finite-difference analogs of the Euler equations, a departure from the exact form has been made. As shown by Forsythe and Wasow (1960, p. 182), the construction of symmetric operators follows directly from the finite-difference form of the functional, Eq. (12) in this case. Assuming that a centered difference is used to approximate $\frac{\partial W}{\partial \sigma}$ in the functional, e.g.,

$$\frac{\partial W}{\partial \sigma}\Big]_{400\ mb} = \frac{W_{250} - W_{700}}{\ln(700/250)}\ , \tag{22}$$

then the finite-difference analog to $\frac{\partial^2 W}{\partial \sigma^2}$ should include values at both the second level above and the second level below the one in question. Because of the limited vertical extend of the discretized analysis space, only the first level above and the first level below are used in calculating the second derivative. This departure from rigorous form introduces some discrepancy between the exact minimum for (12) and the value obtained by using the solution to the assumed finite-difference form of (17)-(19). However, the basic concept of coupling the variables and extrapolation remains intact.

4. METHOD OF SOLUTION

The set of Euler equations are coupled elliptic differential equations (Helmholtz type) subject to Dirichlet conditions. The form of the equation lends itself to a vertically staggered grid arrangement, viz., an alternating sequence of temperature and wind fields along the σ-axis. Equation (19) associates the vertical gradient of vorticity, term (3), and vertical gradient of momentum advection, term (4), with the horizontal temperature distribution. Consequently, the finite-difference evaluation of $\frac{\partial W}{\partial \sigma}$ can be constructed using only the levels adjacent to the temperature. A similar evaluation is possible in connection with (21) and the finite-difference form of $\frac{\partial T}{\partial \sigma}$. A principal advantage of the staggering scheme is the reduction in both computer memory and time requirements.

The staggered system with the assignments for temperature and wind is shown in Fig. 1. The operational sequence of events in the analysis package is (1) the surface wind and pressure field are analyzed by the two-dimensional NVA scheme (Lewis and Grayson, 1972), (2) the SCM upper-air analysis is used for temperature and wind and (3) the variational analysis is accomplished through the solution of (17)-(19). The solution of these Euler equations is schematically represented in Fig. 1.

An elaboration upon the cycling process is instructive:

STEP 1. The 850 mb temperature is found by solving (19) by the accelerated Liebmann method (Miyakoda, 1961). On the first cycle, the available wind field at the adjacent upper level is the SCM analysis.

STEP 2. The 700 mb wind field is found by solving (17) and (18), again by the accelerated Liebmann method. The temperature field at 850 mb found in STEP 1 is now used in conjunction with the SCM temperature analysis at 500 mb to calculate $\frac{\partial T}{\partial \sigma}$. The wind fields at 400 mb (SCM on this first cycle) and the surface are used to estimate $\frac{\partial^2 \mathbb{V}}{\partial \sigma^2}$.

STEP 3. The temperature at 500 mb is found by solving (19), which uses NVA fields below this level and SCM fields above.

STEP 4. The wind field at 400 mb is found by solving (17) and (18), which use NVA fields below and SCM fields above.

STEP 5. The temperature at 300 mb is found by solving (19), which uses the NVA fields at all levels except 250 mb where the wind analysis is derived by the SCM scheme.

With the completion of this complete cycle through the σ-layers, a re-cycling process is performed. Now, the adjusted fields from the first cycle are used as forcing functions in

(17)-(19). As expected, the convergence of the Liebmann method is much faster during the re-cycling (see Table 3). The nonlinear advection terms, $\tilde{A}$ and $\tilde{B}$, are also re-calculated and these improved estimations are used in (17)-(19). The process of re-cycling could be continued indefinitely but obviously at the expense of computer time.

One re-cycle through the levels accounts for most of the adjustment which is fortunate from an operational viewpoint. A more rigorous criterion for termination could be based upon the ratios of observational to dynamical weight. Thus, having specified σ_w/σ_t and σ_T/σ_t beforehand, the final analysis should approach these ratios as the number of cycles increases.

5. APPLICATION

The analysis scheme has been tested using data collected on 15 February 1972. Although the objective analysis was performed over the entire grid (~7000 points at each level), the synoptic discussion will concentrate on the Pacific Ocean region between 20 and 60N. The jet-aircraft flights between the Pacific islands and mainland (Asia and North America) provide credible winds for the upper boundary condition. Additionally, the ship traffic and island density anchor the surface analysis.

Figure 2 depicts the sea level pressure analysis via two-dimensional NVA (Lewis and Grayson, 1972). The data coverage is uniformly dense and both pressure and wind reports have been superimposed over the pressure pattern. The surface wind analysis obtained simultaneously by the NVA scheme is shown in Fig. 3. This analysis serves as the lower boundary condition for the construction of the upper air analysis. The wind has been expressed in knots to conform with the standard operational format.

The upper boundary condition is the SCM analysis of wind at 250 mb. This field is displayed in Fig. 4 and wind observations incorporated into this analysis are shown in Fig. 5. The primitive equation forecast (12 hr) is used as the guess and accounts for the definition of features in data-void areas. For example, the pronounced ridge near

160-170E and extending from 30-45N is virtually the unadulterated guess field.

With the specification of the boundary conditions and the assignment of the weight ratios $\tilde{\alpha}/\alpha$ and $\tilde{\beta}/\alpha$, the Euler equations can be solved. The solution is accomplished by using the accelerated Liebmann method in the level-by-level sequence discussed in Chapter 4. The convergence rate of this iterative method is strongly dependent upon the weight ratios. As $\tilde{\beta}/\alpha$ and $\tilde{\alpha}/\alpha$ increase, the rate of convergence increases. Essentially, term (2) in both (19) and (21) becomes increasingly important and the coupling between the wind and temperature is weakened. Operationally, the range of values for these ratios must be restricted to prevent the usage of unreasonable amounts of computer time. The chosen ratios, however, should guarantee a feedback or coupling between the wind and temperature. The results discussed in this paper have been obtained with the following ratios:

$$\tilde{\alpha}/\alpha = \sigma_t/\sigma_w = 1.5$$
$$\tilde{\beta}/\alpha = \sigma_t/\sigma_T = 250 \qquad (23)$$

where the implied space, time and temperature units are n mi, hr and °C, respectively.

In order to attach physical meaning to these weights, the root-mean-square difference between the SCM fields and

the adjusted fields must be examined. Representative values at 500 mb and 700 mb are displayed in Table 1. It is significant from an operational viewpoint that the major adjustment occurs within two complete cycles through the σ-layers. This table also depicts the root-mean-square value of the shear tendency, S(F) and S(G). Since $\Delta\sigma \sim 0.9$ for the layer between the surface and 400 mb, values of S(F) and S(G) can be roughly interpreted as the 400-1000 mb wind shear change over a one hr period.

A measure of the overall convergence (distinguished from the convergence at a particular level on a given cycle) can be formulated in terms of the difference between calculated and hypothetical ratios. From the form of (12) and the definitions for the weights given in (13), the following relationship should hold:

$$\tilde{\beta}^{-1}: \tilde{\alpha}^{-1}: \tilde{\alpha}^{-1}: \alpha^{-1}: \alpha^{-1} = S^2(T):S^2(u):S^2(v):S^2(F):S^2(G) \tag{24}$$

where S is the root-mean-square designator. From (24) we get

$$\tilde{\beta}/\alpha \begin{cases} = [S(F)/S(T)]^2 \\ = [S(G)/S(T)]^2 \end{cases} \tag{25}$$

and

$$\tilde{\alpha}/\alpha \begin{cases} = [S(F)/S(u)]^2 \\ = [S(F)/S(v)]^2 \\ = [S(G)/S(u)]^2 \\ = [S(G)/S(v)]^2 \end{cases} \tag{26}$$

Average values of $\tilde{\alpha}/\alpha$ and $\tilde{\beta}/\alpha$ based on (25) and (26) are displayed in Table 2. The marked improvement within two cycles is evident. However, the theoretical values can never be obtained because of the truncation error introduced by the finite difference analogs to (17)-(19). Additionally, the license used to formulate the second derivative in terms of adjacent levels (see end of Chapter 3) ultimately causes some discrepancy.

As expected a priori, the amount of computer time necessary to solve for u, v or T at a particular level decreases with every cycle through the σ-layers. Table 3 shows the number of iterations for both temperature and wind at 500 and 700 mb, respectively. The convergence criterion was established to yield solutions accurate to 10^{-2} - 10^{-1}°C and 10^{-1} - 1 kt for temperature and wind, respectively. These values are substantially below the accuracy of the observations.

In order to reveal the magnitude of adjustment in the wind field, a vector difference between the NVA and SCM

analyses is displayed. Figures 6-7 show the vector difference at 700 and 400 mb, respectively, after two complete cycles through the σ-layers. The SCM analysis at 700 and 400 mb is shown in Figs. 8 and 9, respectively. An encouraging result that appears on both Figs. 6 and 7 is the organization of the adjustment. That is, the scale of the adjustment is the same order of magnitude as the synoptic scale disturbances and does not exhibit two or three mesh-length oscillations.

The maximum adjustment at 700 mb occurred in connection with the cyclone at approximately 40N, 175W. The SCM analysis shows definite cyclonic circulation above the surface low pressure center, but the adjustment basically increases the intensity of this vorticity center. Whereas the SCM analysis indicates wind speeds the order of 10 kt to the west of the center, the NVA scheme has speeds around 30 kt. There were no 700 mb observations in this area to verify the adjustment, but the strength of the surface system lends support to both the sense and magnitude of the modification. Another interesting adjustment occurred east of the Japanese Islands in the vicinity of the col in the sea level pressure. The magnitude of 700 mb wind above this area is decreased by NVA and the cyclonic vorticity is weakened. The cyclonic vorticity is increased, however, directly above the two low pressure systems. Generally, the circulations at the surface have been incorporated into the 700 mb chart.

The scale of adjustment at 400 mb appears to be larger than at 700 mb as expected. For example, the upper-air circulation accompanying the mid-Pacific low is adjusted in the cyclonic sense but over a much larger east-west extent. A conspicuous amplification of the ridge along 145W can be seen by examination of the 400 mb adjustment field. Again, this seems to reflect the feedback of information from 250 mb.

The coupling between the temperature and wild fields is displayed in Fig. 10. If the model constraints were strictly geostrophic-hydrostatic, the direction of the shear vector would be along the isotherms and its magnitude would be proportional to the isotherm gradient. There are some noticeably ageostrophic regions especially in the vicinity of weak thermal gradients. The correlation between the shear and the thermal pattern is evident in the baroclinic regions, e.g., the extensive SW-NE flow from mid-Pacific to the Canadian border and the SW-NE flow just east of Japan.

With the weight ratios given by (23), the influence of the wind field on the temperature field is not as conspicuous as the reverse coupling, i.e., the influence of temperature on wind. This statement is further substantiated by the results in Table 1 indicating that the NVA temperature

is very close, in an rms sense, to the SCM temperature. Stated mathematically, term (2) in (19) dominates the other terms in this equation. In order to isolate the influence of wind on temperature, an experiment was conducted in which $\tilde{\beta} = 0$. Thus, term (2) vanishes in (19) and the temperature at any level is a function of the wind field and the boundary values of temperature on the north and south walls.

As expected, the rate of convergence is slowed down considerably in this case; in fact, the number of iterations increased by a factor of 7. The 850 mb temperatures for the case $\tilde{\beta} = 0$ and the control case, i.e., weights given by (23), are shown in Figs. 11 and 12, respectively. The maximum or minimum values or "central" values are in obvious disagreement. Effectively, the $\tilde{\beta} = 0$ case has no anchoring information on the interior. It is very encouraging, however, to see the coupling between isotherm curvature and the wind shear vector. Especially interesting is the cut-off feature in mid-Pacific.

6. CONCLUDING REMARKS

The primary results based on this study are (1) the variational method can incorporate detail into the 400-700 mb wind fields via vertical coupling and (2) the iterative technique for solving the analysis equations is efficient enough to withstand the rigid time requirements of operational analysis and prediction. Based on information from the case study, the estimated time for solution to the Euler equations is 15 min [Central Processor Unit (CPU)] on the CDC 6500 computer. The SCM analysis takes approximately 15 min also, yielding a combined time of 30 min for the entire analysis. The analysis will be routinely transmitted (every 6 hr) to the outlying weather centers in June, 1972.

Considerable effort is currently concentrated on increasing the data-base for the analysis. In particular: (1) the incorporation of pibals (pilot balloons) information will ultimately strengthen the low-level wind field; (2) the winds derived from satellite photographs will provide support at both the upper-level (~250 mb) and low-level (~700 mb); and (3) temperature information from SIRS soundings will be added to the conventional temperature reports.

TABLE 1. Root-mean-square differences between adjusted fields (NVA) and SCM fields denoted by S(T), S(u) and S(v) where the differences are calculated at 500 mb and 700 mb for the temperature and wind, respectively. The mean-square values of F and G (see Eqs. 7 and 8) at 500 mb are denoted by S(F) and S(G).

Cycle	S(T) °C	S(u) kt	S(v) kt	S(F) kt hr^{-1}	S(G) kt hr^{-1}
1	0.324	3.83	4.34	7.68	5.75
2	0.325	3.82	4.02	6.39	5.12
3	0.323	3.85	4.01	6.20	5.02
4	0.322	3.88	4.03	6.16	5.07

TABLE 2. Ratio between observational and dynamic weight as a function of cycle number. The hypothetical ratios are shown in parentheses and the calculations based on values from TABLE 1.

Cycle	$\frac{\tilde{\alpha}}{\alpha}$ (1.5)	$\frac{\tilde{\beta}}{\alpha}$ (250)
1	2.78	424
2	2.18	327
3	2.06	305
4	2.04	308

TABLE 3. The iterative solution to the Euler equations is accomplished by the accelerated Liebmann method. The number of iterations required for convergence is displayed as a function of the cycle. These numbers represent the calculations at 700 mb and 500 mb for wind and temperature, respectively.

Cycle	Temperature	Wind
1	11	9
2	6	8
3	5	6
4	4	5

REFERENCES

Bergthórsson, P., and B. Döös, 1955: Numerical weather map analysis. Tellus, 7, 329-340.

Cramér, H., 1955: The Elements of Probability Theory. New York, Wiley, 281 pp.

Cressman, G. P., 1959: An operational objective analysis system. Mon. Wea. Rev., 94, 367-374.

Döös, B., 1970: Numerical experimentation related to GARP. Global Atmospheric Research Programme (GARP), WMO-ICSU Joint Organizing Committee, Pub. Ser. No. 6, 32 pp.

Flattery, T. W., 1970: Spectral analysis and forecasting. Numerical Weather Prediction Activities, National Meteorological Center (NMC), Second-half 1969, 51 pp.

Flattery, T. W., 1971: Spectral models for global analysis and forecasting. Proc. 6th AWS Tech. Exch. Conf., U. S. Naval Acad., Air Weather Service Rept. 242, 42-54.

Forsythe, G. E., 1945: A generalization of the thermal wind equation to arbitrary horizontal flow. Bull. of Amer. Meteor. Soc., 26, 371-375.

Forsythe, G. E., and W. R. Wasow, 1960: Finite-Difference Methods for Partial Differential Equations, New York, Wiley, 444 pp.

Kesel, P. G., and F. J. Winninghoff, 1971: Fleet Numerical Weather Central's four processor primitive equation model. Proc. 6th AWS Tech. Exch. Conf., U. S. Naval Acad., Air Weather Service Rept. 242, 17-41.

Lanczos, C., 1970: The Variational Principles of Mechanics, 4th ed. University of Toronto Press, Math Expositions No. 4, 375 pp.

Lewis, J. M., and T. H. Grayson, 1972: The adjustment of surface wind and pressure by Sasaki's variational matching technique. Accepted for publication in J. Appl. Meteor.

Masuda, Y., and A. Arakawa, 1962: On the objective analysis for surface and upper level maps. Proc. Intern. Symp. Numerical Weather Prediction Tokyo, 1960, Meteor. Soc. Japan, 55-66.

Miyakoda, K., 1961: Contribution to numerical weather prediction - computation with finite difference. Geophysical Institute, Tokyo University, 190 pp. (see p. 96).

Sasaki, Y., 1958: An objective analysis based on the variational method. J. Meteor. Soc. Japan, 36, 77-88.

_____, 1969: Proposed inclusion of time variation terms, observational and theoretical, in numerical variational objective analysis. J. Meteor. Soc. Japan, 47, 115-124.

_____, 1970: Some basic formalisms in numerical variational analysis. Mon. Wea. Rev., 98, 875-910.

Saucier, W. M., 1955: Principles of Meteorological Analysis, University of Chicago Press, 438 pp.

Stephens, J. J., 1967: Filtering responses of selected distance dependent weight functions. Mon. Wea. Rev., 95, 45-46.

Wise, C. W., and R. H. Simpson, 1971: The tropical analysis program of the National Hurricane Center, Weatherwise, 24, 164-173.

Yanai, M., 1964: An experimental objective analysis in the tropics. Tech. Paper No. 22, Dept. of Atmos. Sci., Colorado State University, 21 pp.

APPENDIX: NATURAL BOUNDARY CONDITIONS

The right hand side of (15) has categorically grouped the terms involving integrals over the boundary surfaces. These integrals originate from the last set of bracketed terms in (12). The mechanics of extracting the surface integrals from the functional is explained in Lanczos (1970). Before writing the explicit form of these integrals, it is convenient to adopt the following notation:

x', x'' : boundaries of analysis space in east-west direction

y', y'' : boundaries of analysis space in north-south direction

σ', σ'' : boundaries of analysis space in vertical direction

Realizing that the global-band is cyclic in the longitudinal or east-west direction, the relationship

$$\phi(x') = \phi(x'') \tag{A1}$$

holds, where ϕ represents any of the variables, u, v or T or derivatives of these variables. The explicit form is:

$$\left\{\begin{matrix}\text{Boundary}\\ \text{Terms}\end{matrix}\right\} = \alpha R^2 \iint \overset{①}{[\delta T \cdot \frac{\partial T}{\partial x}]_{x'}^{x''}}\, dyd\sigma + \alpha R^2 \iint \overset{②}{[\delta T \cdot \frac{\partial T}{\partial Y}]_{y'}^{y''}}\, dxd\sigma$$

$$+ \frac{\alpha Rf}{m} \iint \overset{③}{[\delta T \cdot \frac{\partial u}{\partial \sigma}]_{y'}^{y''}}\, dxd\sigma - \frac{\alpha Rf}{m} \iint \overset{④}{[\delta T \cdot \frac{\partial v}{\partial \sigma}]_{x'}^{x''}}\, dyd\sigma$$

$$+ \frac{\alpha R}{m} \iint \overset{⑤}{[\delta T \cdot \frac{\partial \tilde{B}}{\partial \sigma}]_{y'}^{y''}}\, dxd\sigma + \frac{\alpha R}{m} \iint \overset{⑥}{[\delta T \cdot \frac{\partial \tilde{A}}{\partial \sigma}]_{x'}^{x''}}\, dyd\sigma \qquad \text{(A2)}$$

$$+ \frac{\alpha Rf}{m} \iint \overset{⑦}{[\delta u \cdot \frac{\partial T}{\partial y}]_{\sigma'}^{\sigma''}}\, dxdy - \frac{\alpha Rf}{m} \iint \overset{⑧}{[\delta v \frac{\partial T}{\partial x}]_{\sigma'}^{\sigma''}}\, dxdy$$

$$+ \frac{\alpha f^2}{m^2} \iint \overset{⑨}{[\delta u \frac{\partial u}{\partial \sigma}]_{\sigma'}^{\sigma''}}\, dxdy + \frac{\alpha f^2}{m^2} \iint \overset{⑩}{[\delta v \cdot \frac{\partial v}{\partial \sigma}]_{\sigma'}^{\sigma''}}\, dxdy$$

$$+ \frac{\alpha f}{m^2} \iint \overset{⑪}{[\delta u \cdot \frac{\partial \tilde{B}}{\partial \sigma}]_{\sigma'}^{\sigma''}}\, dxdy - \frac{\alpha f}{m^2} \iint \overset{⑫}{[\delta v \cdot \frac{\partial \tilde{A}}{\partial \sigma}]_{\sigma'}^{\sigma''}}\, dxdy$$

where $[\phi(x,y,\sigma)]_{x'}^{x''} = \phi(x'',y,\sigma) - \phi(x',y,\sigma)$ in conformity with notation of integral calculus. The terms ①, ④ and ⑥ vanish by virtue of (A1). If $\delta T = 0$ along the north and south walls, then ②, ③ and ⑤ vanish. When $\delta u = \delta v = 0$ on the upper and lower boundaries, then terms ⑦ - ⑫ vanish. These are the Dirichlet conditions for the formulation and they have been adopted.

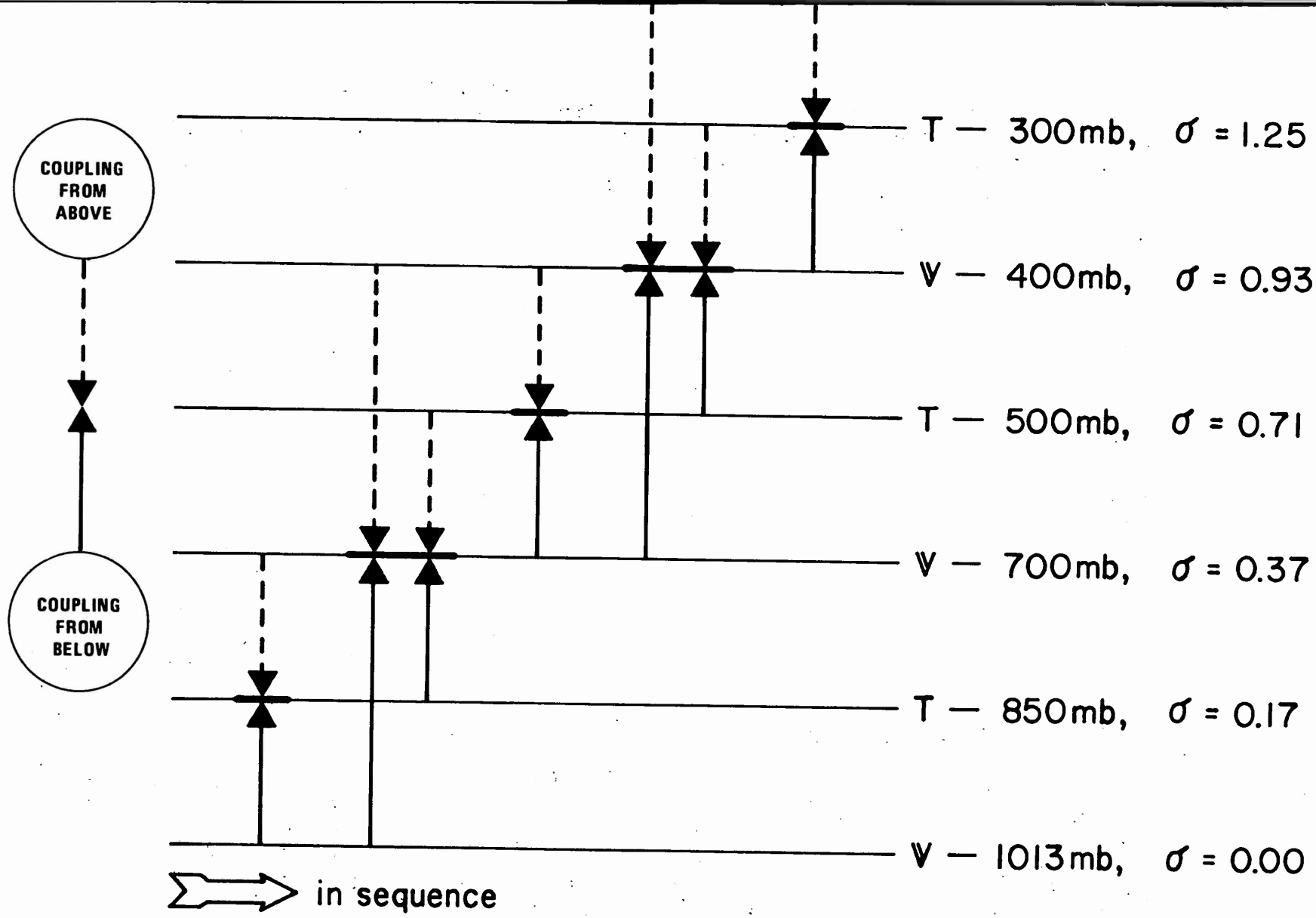

Figure 1: Schematic representation of "Ascent-Cascade" process of upper-air analysis. The fields at the surface and 250 mb are control or anchor levels. Analysis begins at 850 mb and proceeds to 300 mb (sequencing from bottom to top and left to right in the figure). After completion of a cycle from 850 to 300 mb, the procedure is repeated using the adjusted values as input.

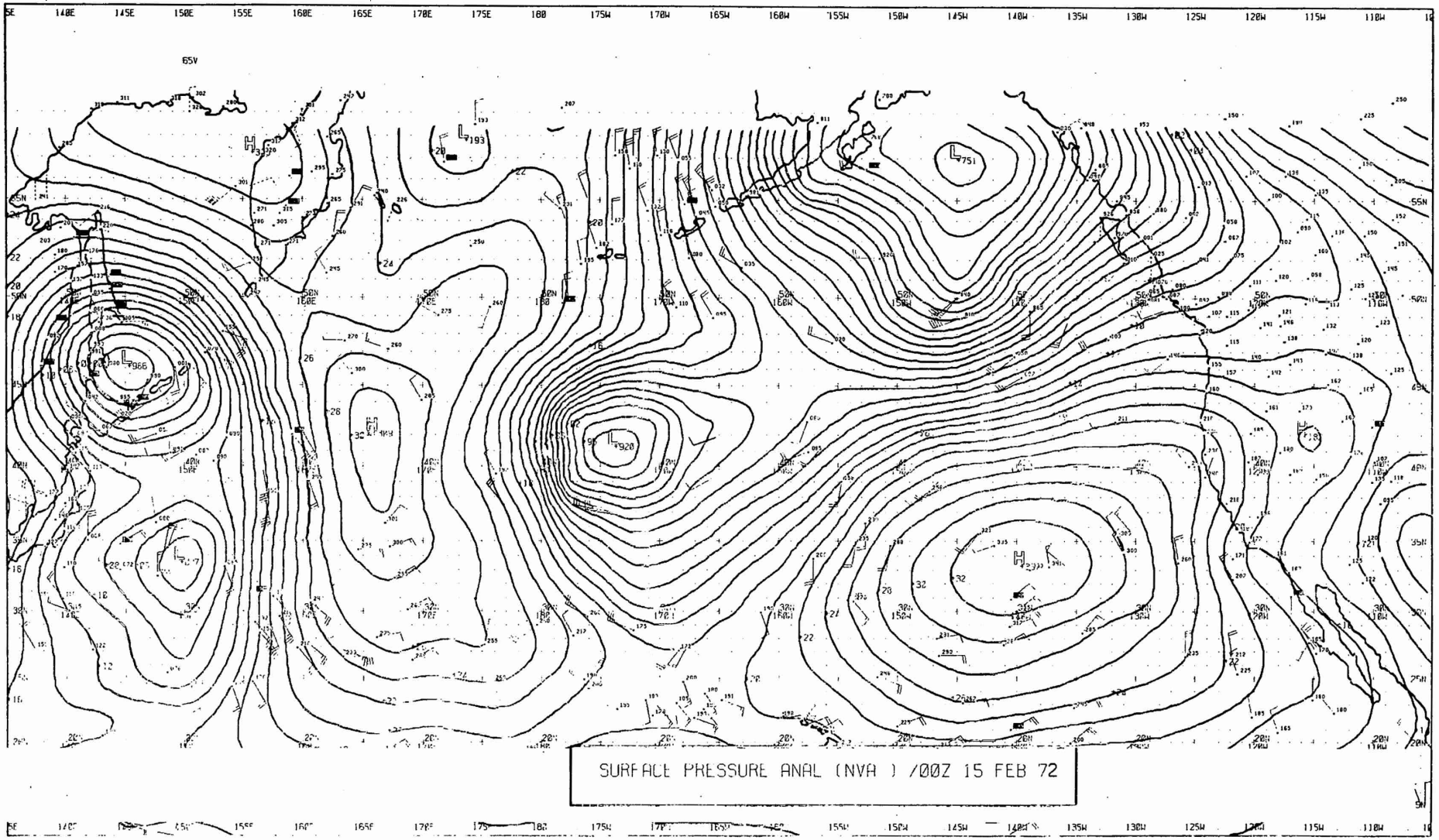

Figure 2: Sea level pressure at 00Z on 15 February 1972. This analysis is the result of a two-dimensional NVA adjustment that has incorporated both wind and pressure reports. The observed wind (knots) and pressure (tenths of a millibar) rejected during analysis have been denoted by dotted barbs and blocked numbers, respectively.

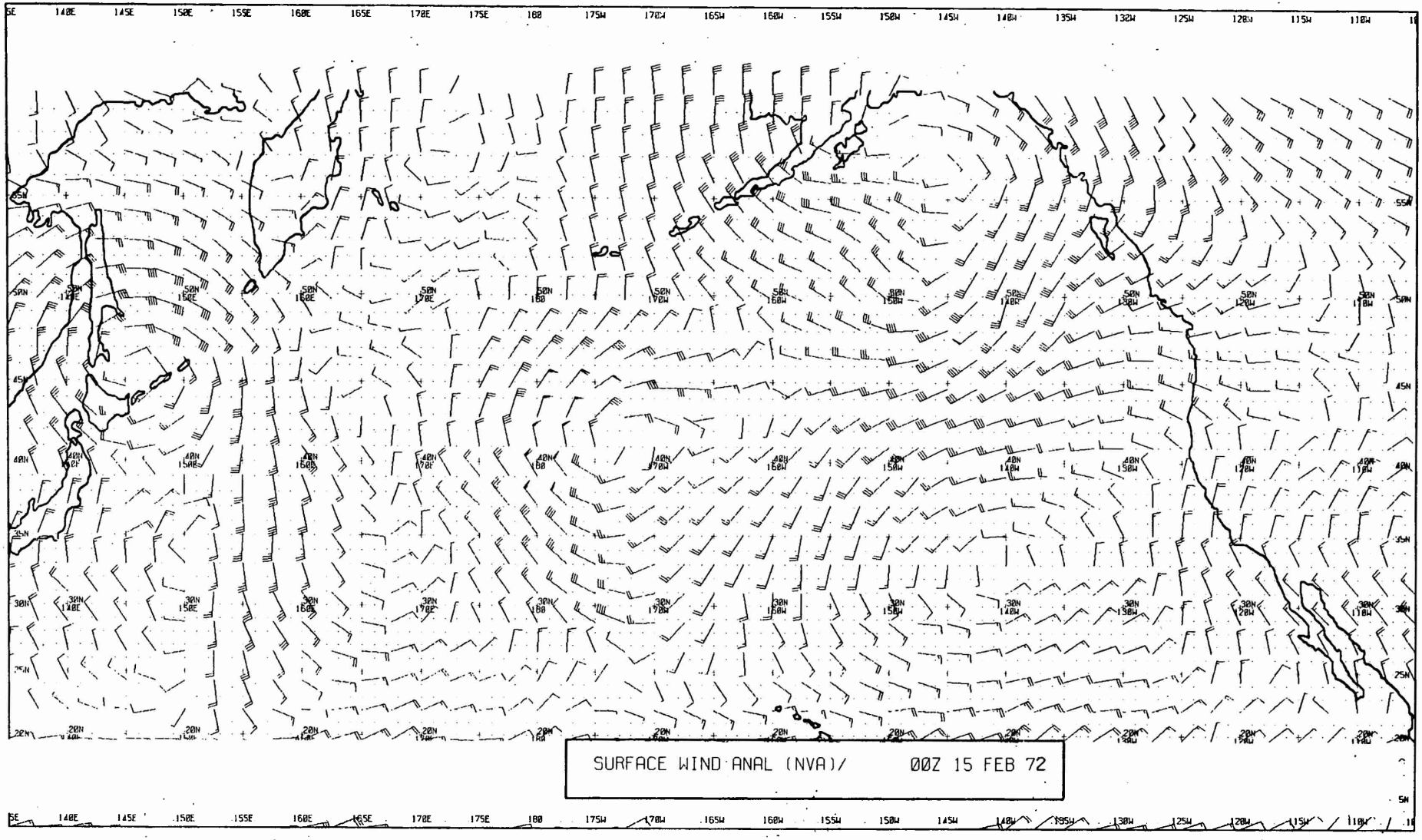

Figure 3: Surface winds (knots) obtained in conjunction with the pressure analysis is shown in Fig. 1. This variational analysis served as the lower boundary condition for the construction of the upper-air wind and temperature fields.

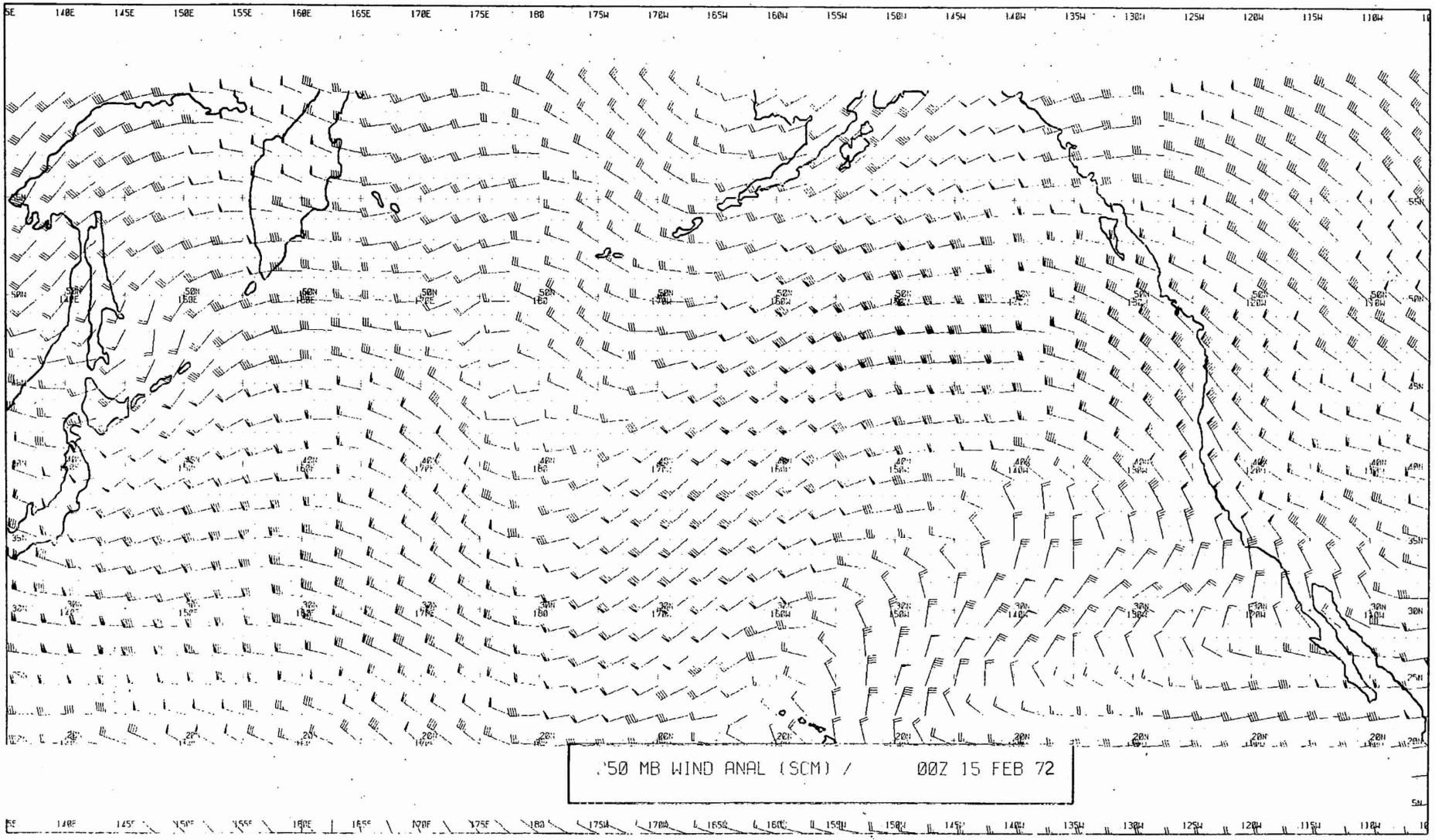

Figure 4: 250 mb winds (knots) which serve as the upper boundary condition for construction of the intermediate levels. This analysis is derived by the SCM scheme and has not been subjected to variational adjustment.

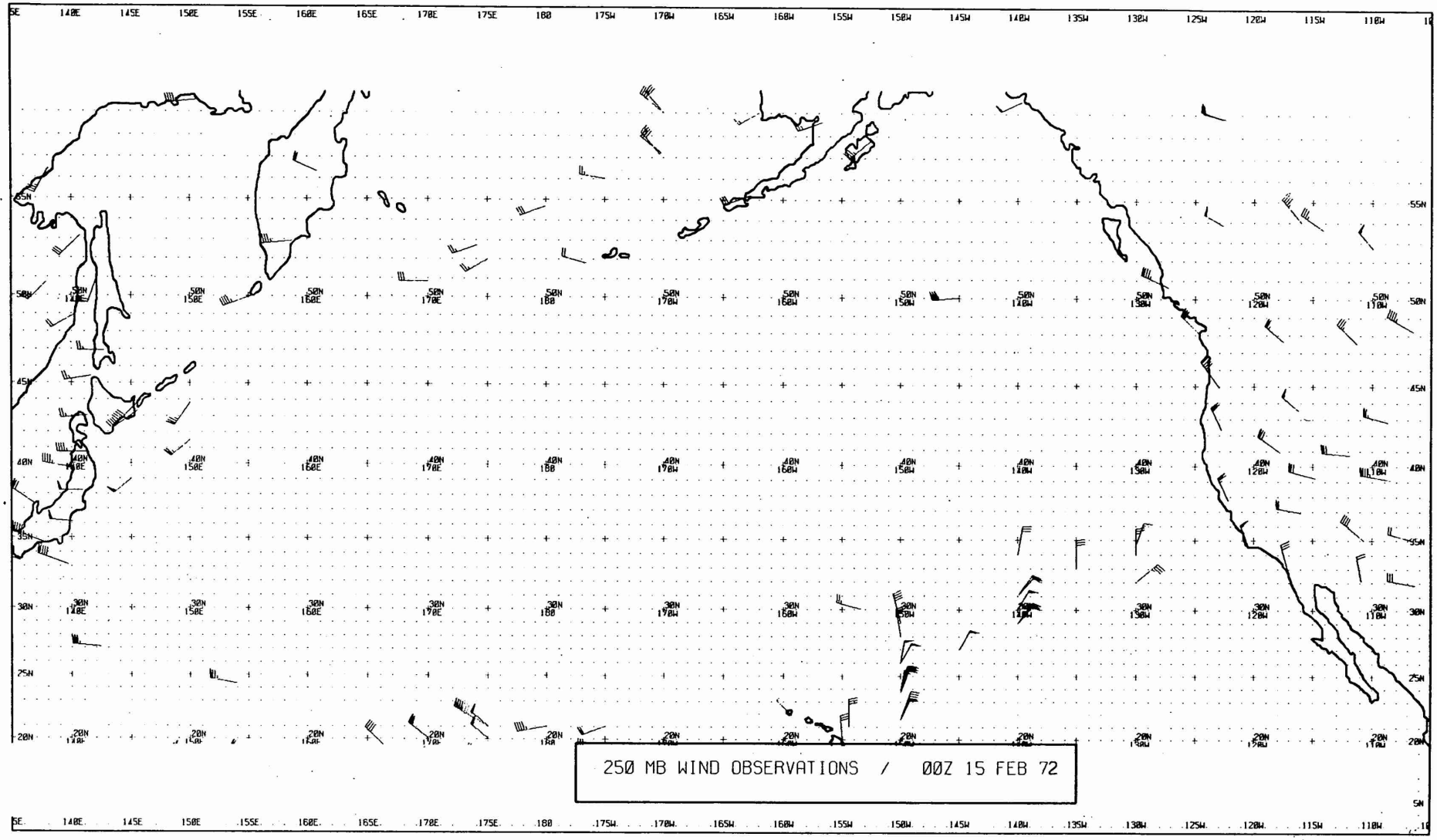

Figure 5: The wind observations (knots) used by the SCM scheme to construct the 250 mb analysis. The guess field for the SCM above 20N is the 12-hr forecast from the primitive equation model.

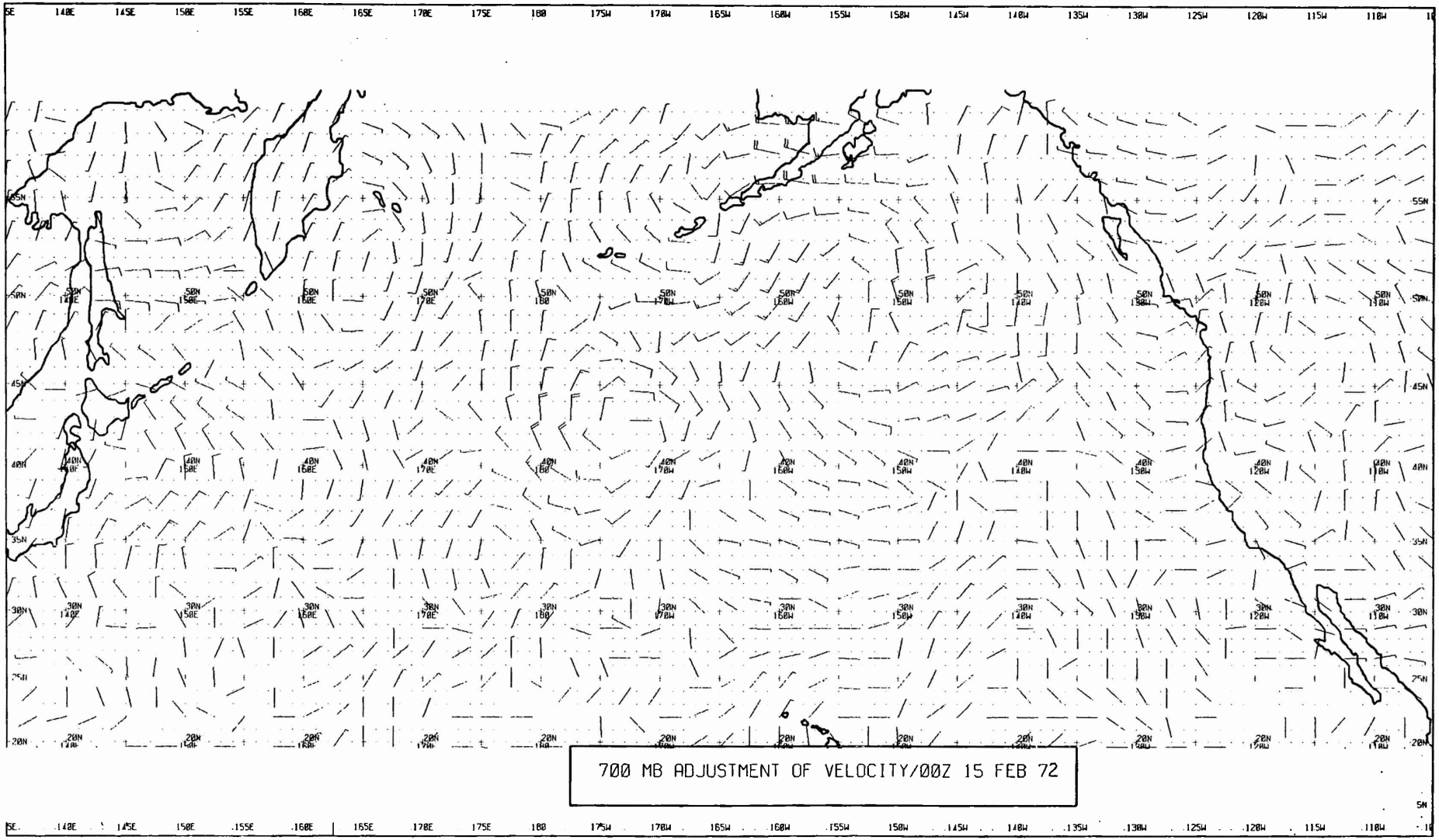

Figure 6: Vector difference between the NVA velocity and SCM velocity at 700 mb, $\mathbb{V} - \tilde{\mathbb{V}}$. This vector represents the adjustment after two cycles of the Ascent-Cascade process.

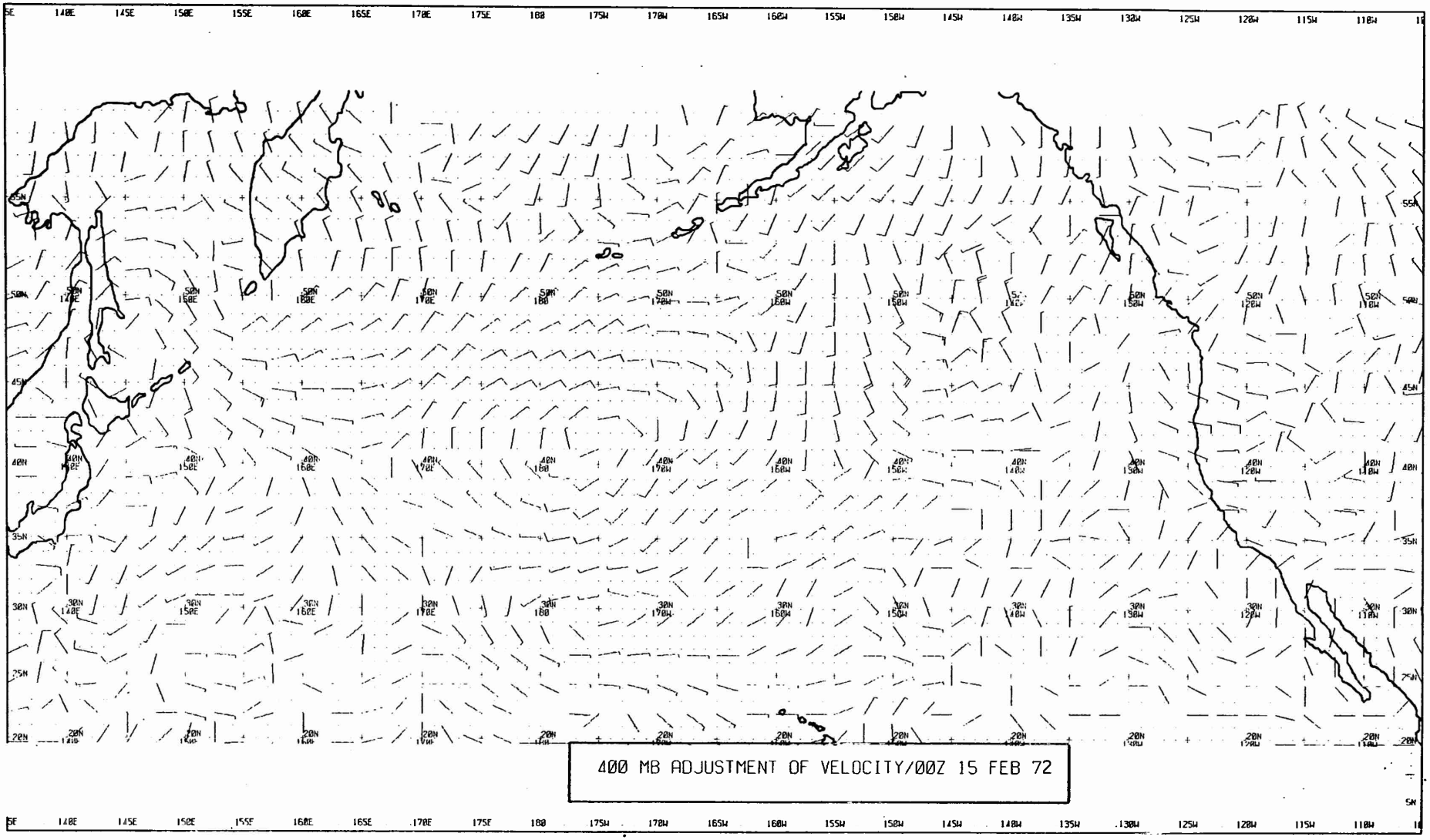

Figure 7: Vector difference between the NVA velocity and SCM velocity at 400 mb, $\vec{V} - \tilde{V}$. This vector represents the adjustment after two cycles of the Ascent-Cascade process.

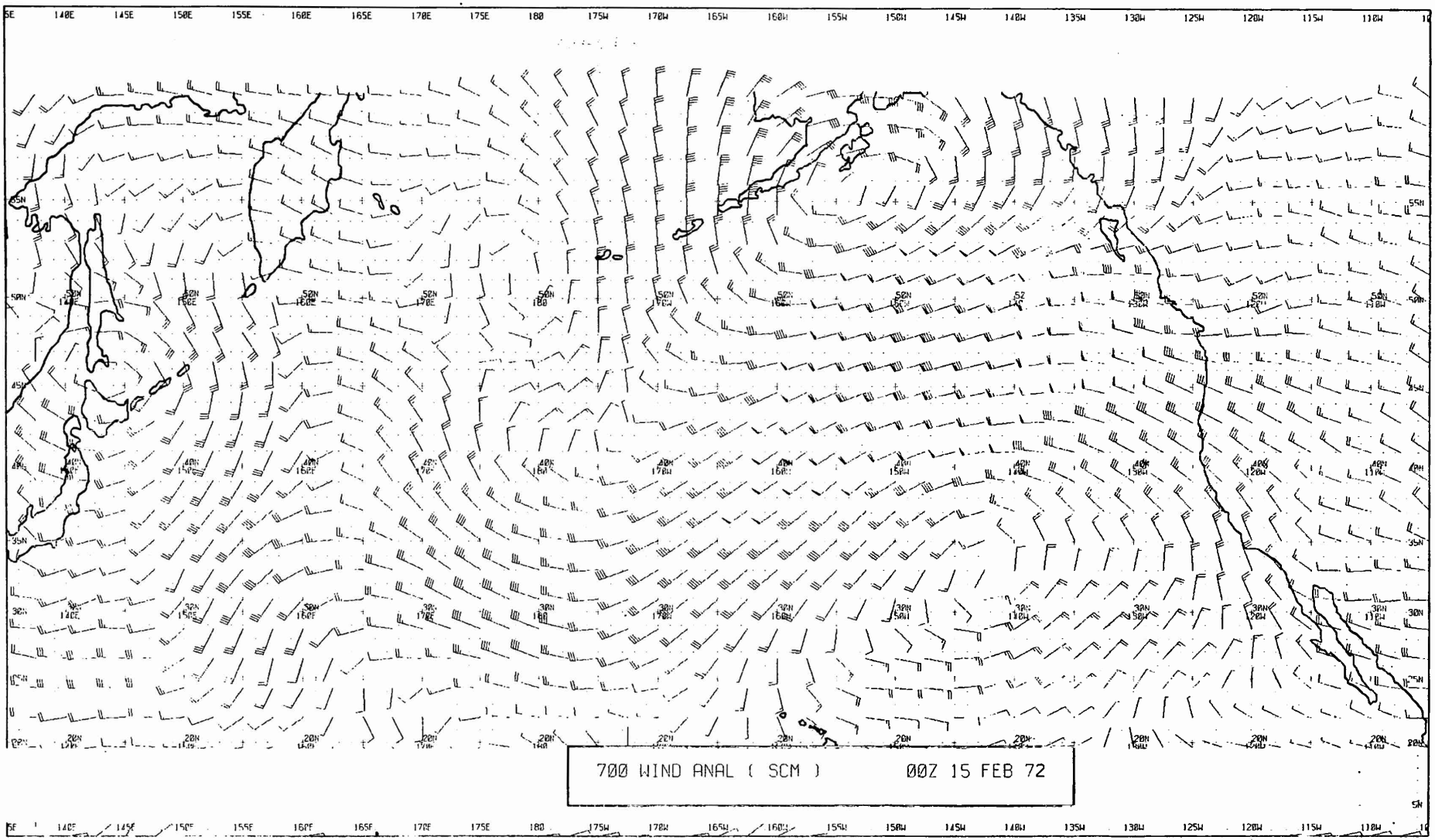

Figure 8: 700 mb wind analysis (knots) by SCM scheme, $\tilde{V}$(700mb).

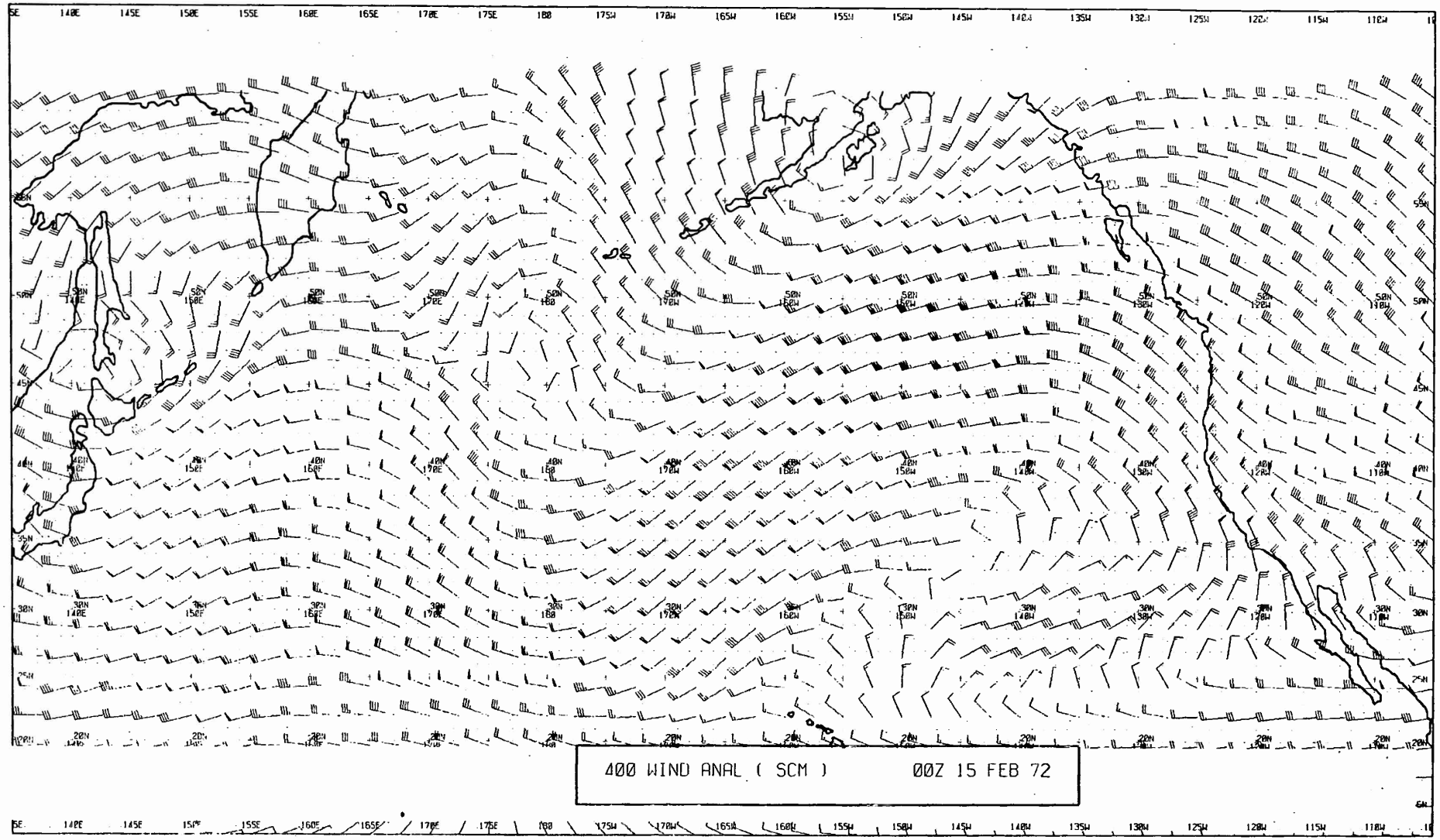

Figure 9: 400 mb wind analysis (knots) by SCM scheme, $\tilde{W}$(400mb).

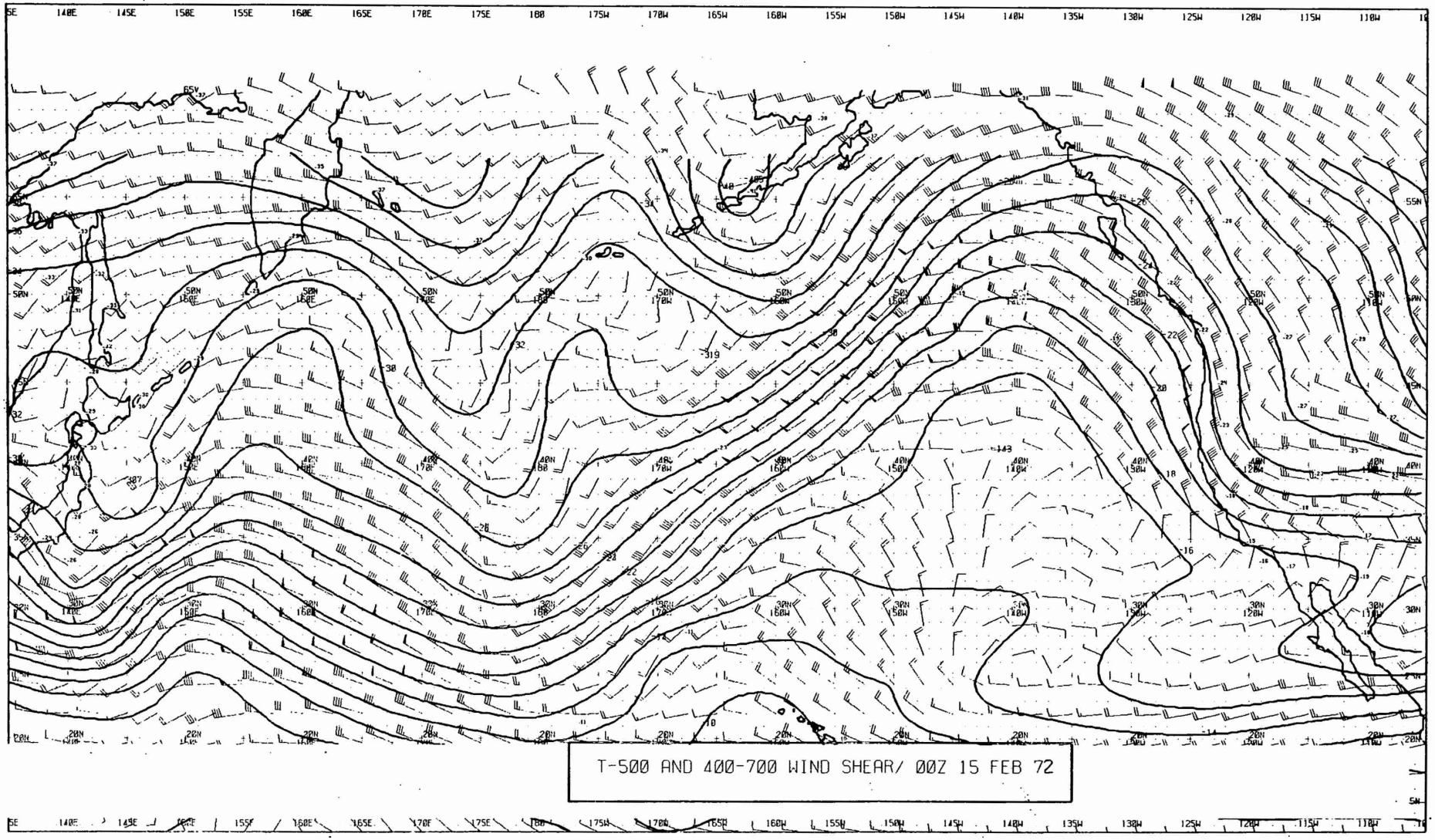

Figure 10: Wind shear (knots) between 400 and 700 mb, W(400) - W(700), superimposed on the temperature field at 500 mb. Observed temperatures used in the analysis have been denoted on the figure.

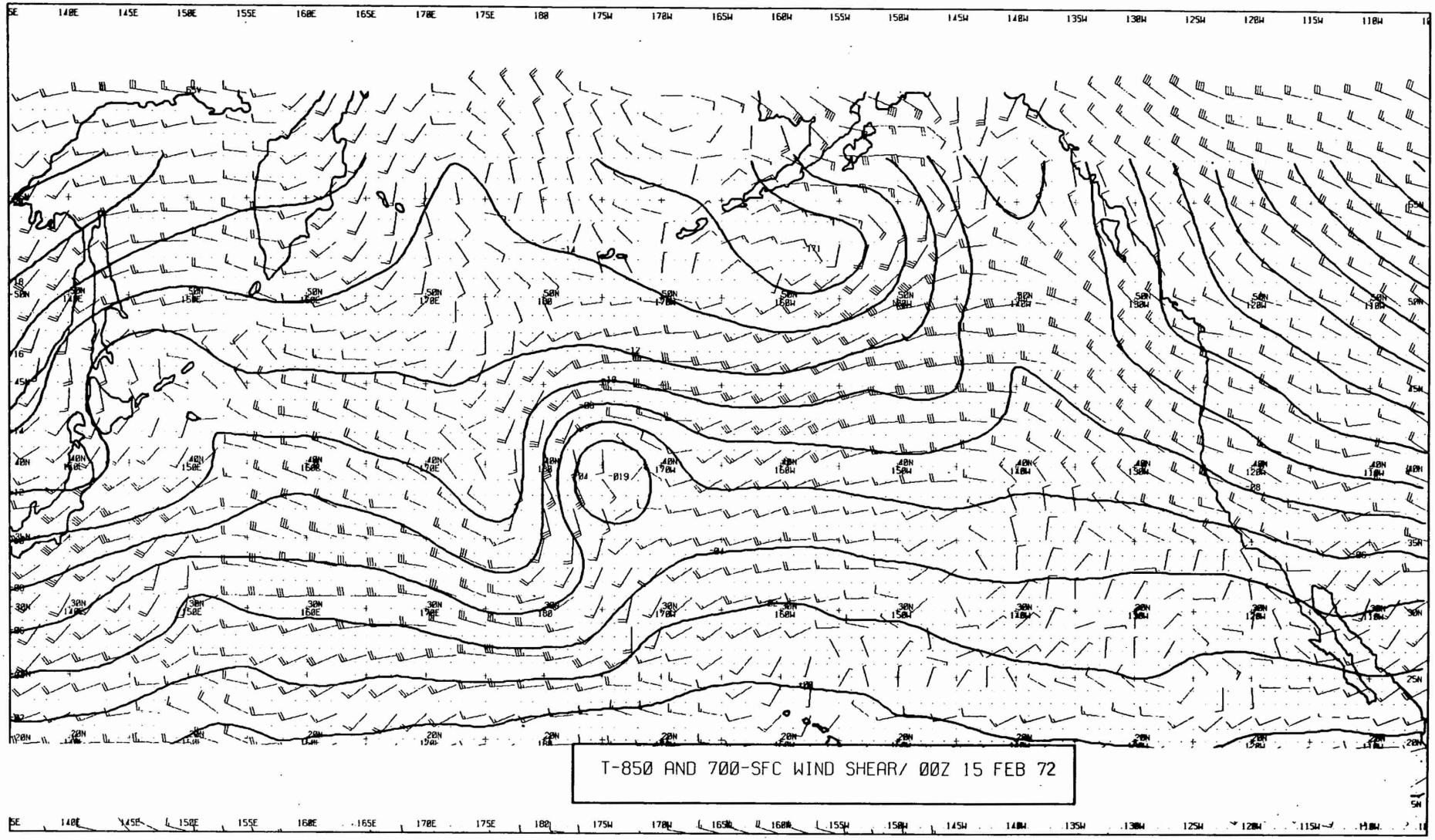

Figure 11: Wind shear (knots) between 700 mb and the surface $V(700) - V(SFC)$, superimposed on the temperature field at 850 mb. This analysis used $\tilde{\beta} = 0$.

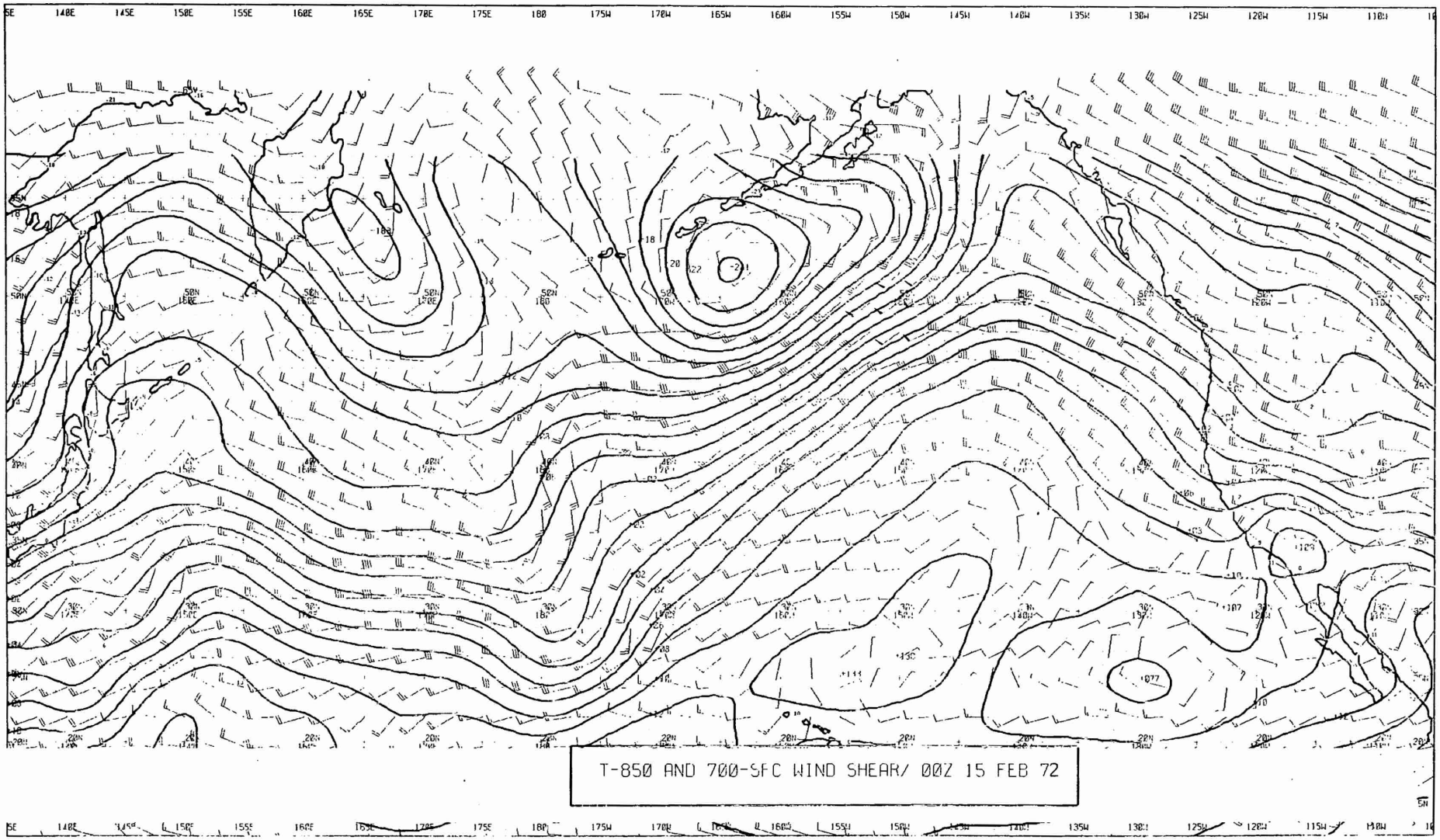

Figure 12: Same as Fig. 11 except weights used in accord with Eq. (23).

UNCLASSIFIED
Security Classification

DOCUMENT CONTROL DATA - R & D

(Security classification of title, body of abstract and indexing annotation must be entered when the overall report is classified)

1. ORIGINATING ACTIVITY *(Corporate author)*

Fleet Numerical Weather Central

2a. REPORT SECURITY CLASSIFICATION

Unclassified

2b. GROUP

3. REPORT TITLE

An Operational Upper Air Analysis Using the Variational Method

4. DESCRIPTIVE NOTES *(Type of report and inclusive dates)*

Technical Note No. 72-3, May 1972

5. AUTHOR(S) *(First name, middle initial, last name)*

John M. Lewis

6. REPORT DATE	7a. TOTAL NO. OF PAGES	7b. NO. OF REFS
May 1972	50	20

8a. CONTRACT OR GRANT NO.	9a. ORIGINATOR'S REPORT NUMBER(S)
b. PROJECT NO.	
c.	9b. OTHER REPORT NO(S) *(Any other numbers that may be assigned this report)*
d.	

10. DISTRIBUTION STATEMENT

Approved for public release; distribution unlimited.

11. SUPPLEMENTARY NOTES	12. SPONSORING MILITARY ACTIVITY

13. ABSTRACT

An upper air objective analysis of wind and temperature has been developed for operational use at Fleet Numerical Weather Central. The primary feature of this analysis scheme is the vertical and horizontal extrapolation of information into the data-sparse regions from the data-rich surface and jet aircraft level. The extrapolation is based on Sasaki's recent extensions of the variational analysis method. The hydrostatic equation and horizontal momentum equations are used as dynamical constraints and these equations are combined to relate temperature and wind through a generalized thermal wind relationship. The governing analysis equations are elliptic and amenable to solution by the relaxation process. Vertical coupling of both wind and temperature is demonstrated through the detailed examination of a case study in the North Pacific.

DD FORM 1 NOV 65 1473 (PAGE 1)

S/N 0101-807-6801

UNCLASSIFIED
Security Classification

14. KEY WORDS	LINK A		LINK B		LINK C	
	ROLE	WT	ROLE	WT	ROLE	WT
Numerical Variational Analysis (NVA)						
Upper-Air Analysis						
Global-band grid						
Objective Analysis						
Tropical Analysis						
General thermal wind constraint						
Coupling between wind and temperature analysis